Structural and mechanistic basis behind the inhibitory interaction of PcTS on α-synuclein amyloid fibril formation

Gonzalo R. Lamberto[a], Andrés Binolfi[a], María L. Orcellet[a], Carlos W. Bertoncini[b], Markus Zweckstetter[c,d], Christian Griesinger[c], and Claudio O. Fernández[a,c,1]

[a]Instituto de Biología Molecular y Celular de Rosario, Consejo Nacional de Investigaciones Científicas y Técnicas, Universidad Nacional de Rosario, Suipacha 531, S2002LRK Rosario, Argentina; [b]Department of Chemistry, University of Cambridge, Lensfield Road, CB2 1EW Cambridge, United Kingdom; [c]Department of Nuclear Magnetic Resonance-Based Structural Biology, Max Planck Institute for Biophysical Chemistry, Am Fassberg 11, D-37077 Göttingen, Germany; and [d]Deutsche Forschungsgemeinschaft Center for the Molecular Physiology of the Brain, D-37077 Göttingen, Germany

Edited by Joan Selverstone Valentine, University of California, Los Angeles, CA, and approved October 16, 2009 (received for review March 9, 2009)

The identification of aggregation inhibitors and the investigation of their mechanism of action are fundamental in the quest to mitigate the pathological consequences of amyloid formation. Here, characterization of the structural and mechanistic basis for the antiamyloidogenic effect of phthalocyanine tetrasulfonate (PcTS) on α-synuclein (AS) allowed us to demonstrate that specific aromatic interactions are central for ligand-mediated inhibition of amyloid formation. We provide evidence indicating that the mechanism behind the antiamyloidogenic effect of PcTS is correlated with the trapping of prefibrillar AS species during the early stages of the assembly process. By using NMR spectroscopy, we have located the primary binding region for PcTS to a specific site in the N terminus of AS, involving the amino acid Tyr-39 as the anchoring residue. Moreover, the residue-specific structural characterization of the AS-PcTS complex provided the basis for the rational design of nonamyloidogenic species of AS, highlighting the role of aromatic interactions in driving AS amyloid assembly. A comparative analysis with other proteins involved in neurodegenerative disorders reveals that aromatic recognition interfaces might constitute a key structural element to target their aggregation pathways. These findings emphasize the use of aggregation inhibitors as molecular probes to assess structural and toxic mechanisms related to amyloid formation and the potential of small molecules as therapeutics for amyloid-related pathologies.

aggregation inhibitor | misfolding | Parkinson's disease

The misfolding of proteins into a toxic conformation is proposed to be at the molecular foundation of a number of neurodegenerative disorders, including Creutzfeldt–Jacob's, Alzheimer's, and Parkinson's disease (PD) (1). One common and defining feature of protein misfolding diseases is the formation and deposition of amyloid-like fibrils. Neurodegeneration in PD is progressive and characterized by the loss of dopaminergic neurons in the substantia nigra and the presence of fibrillar cytoplasmic aggregates of the protein α-synuclein (AS) in multiple brain regions (2). Evidence that AS amyloidogenesis has a causative role in the development of PD is furnished by a variety of genetic, neuropathological, and biochemical studies (3, 4). The detailed understanding of the phenomenon of AS amyloid fibrillation and its inhibition is therefore highly clinically important.

Structurally, AS comprises 140 amino acids distributed in three different regions: the amphipathic N terminus (residues 1–60), showing the imperfect KTKEGV repeats and involved in lipid binding; the highly hydrophobic self-aggregating sequence known as nonamyloid component (NAC) (residues 61–95), which is presumed to initiate fibrillation (5); and the acidic C-terminal region (residues 96–140), rich in Pro, Asp, and Glu residues and critical for blocking rapid AS filament assembly (Fig. 1) (6). In its native monomeric state AS adopts an ensemble of conformations with no rigid secondary structure although long-range interactions have been shown to stabilize an aggregation-autoinhibited conformation (7–9). The precise function of AS is unknown, as are the mechanism(s) underlying the structural transition from the innocuous, monomeric conformations of AS to its neurotoxic forms.

Currently, no preventive therapy is available for PD and related synucleinopathies. Identification of therapeutic drugs is not only complicated by a lack of understanding of many of the key aspects of PD pathogenesis but also by the multifactorial etiology of the disease. The aggregation pathway of AS represents then an obvious target for therapeutic intervention in PD. Indeed, one approach to the development of therapeutic agents in neurodegenerative diseases has been the use of small molecules that specifically and efficiently inhibit the aggregation process. From these studies, a range of small compounds demonstrated to inhibit the formation of fibrillar aggregates of amyloid proteins such as Aβ (10–13), tau (14), huntingtin (15), and prion protein (16, 17). Although less well defined, studies focused on small molecule inhibitors of AS filament assembly are becoming an active area of research (13, 18–24). The flavonoid baicalein was shown to inhibit the fibrillation of AS and disaggregate existing mature fibrils (20, 23), whereas a series of different chemical compounds (13, 18, 19) led to the formation of soluble oligomeric species that were not toxic to nerve cells. More recently, NMR spectroscopy revealed some structural and molecular details of the interaction of AS with the polyphenol EGCG and with a number of aggregation inhibitory compounds (13, 22). The polyphenol EGCG was suggested to inhibit AS fibrillation by directly binding to the C terminus of natively unfolded AS monomers and stimulating its assembly into nontoxic oligomers that were said to be off-pathway (13). By contrast, other inhibitors such as Congo red and lacmoid were shown to interact essentially with the entire amphipathic AS region, reminiscent of the protein interaction with detergent micelles and lipid vesicles (22). Unfortunately, the extensive broadening that the studied compounds caused on the backbone resonances of AS impaired the identification of the residues involved in the interaction (13, 22). The access to such information is not only paramount for drug development but also to understand the molecular basis of AS amyloid formation.

In this work, we report high-resolution structural information of the interaction between AS and the cyclic tetrapyrrole phthalocyanine tetrasulfonate (PcTS) (Fig. S1*C*). This compound was previously shown to exhibit antiscrapie activity in vitro and in vivo (16, 17), disassembling of tau filaments (14), and inhibition of AS

Author contributions: G.R.L. and C.O.F. designed research; G.R.L., A.B., M.L.O., and C.W.B. performed research; G.R.L., A.B., M.L.O., C.W.B., and C.O.F. analyzed data; and G.R.L., C.W.B., M.Z., C.G., and C.O.F. wrote the paper.

The authors declare no conflict of interest.

This article is a PNAS Direct Submission.

[1]To whom correspondence should be addressed. E-mail: fernandez@ibr.gov.ar.

This article contains supporting information online at www.pnas.org/cgi/content/full/0902603106/DCSupplemental.

Fig. 1. Alignment of the AS and BS amino acids sequences. BS lacks the central hydrophobic NAC region, whereas AS has a shorter C terminus. Shaded in light gray are amino acids that differ between both proteins. Aromatic residues are shaded in dark gray at the N-terminal and NAC regions, and in black at the C terminus.

filament assembly, leading to the formation of nontoxic AS aggregates (21). The strategy used in this work allowed us to demonstrate unequivocally that PcTS inhibition of AS amyloid fibril formation is mediated via specific binding to aromatic residues in the N-terminal region of the protein. The elucidation of the structural details of this interaction shed new light into the fibrillation pathway of AS and the mechanistic basis that direct the inhibitory effect.

Results

PcTS-Mediated Inhibition of AS Amyloid Fibril Formation. As previously reported, the cyclic tetrapyrrole PcTS was able to impair the ability of AS to form amyloid fibrils in a concentration-dependent manner (21). Notably, we found that PcTS did not significantly reduce the amount of aggregated AS; however, the presence of AS deposits with the characteristic amyloid morphology was greatly diminished as a function of the concentration of PcTS (Fig. S1 *A* and *B*). Instead, a variety of smaller, apparently amorphous, nonfibrillar AS species, as well as short, flat fibrillar AS aggregates, were favored by the presence of the ligand, as observed by transmission electron microscope (TEM) (Fig. S1*B*). Interestingly, PcTS was mostly incorporated into AS aggregates, as revealed by absorption spectroscopy on extensively washed samples (Fig. S1*C*).

Biophysical studies on PcTS induced aggregates show that, contrary to amyloid fibrils of AS, these formations are more sensitive to dissolution by the mild detergent Sarkosyl and have a reduced β-sheet signature, as measured by CD (Fig. 2*A*). No evidence of SDS-insoluble AS oligomers, typical of stable off-pathway intermediates, was found in PcTS inhibited assembly reactions (13). Furthermore, PcTS-induced AS aggregates were still capable of seeding amyloid formation of AS, although with much less efficiency than ligand-free mature AS deposits (Fig. 2*B*). No major changes were observed in the rate of aggregation growth (k_{app}) between the seeding experiments using PcTS generated AS aggregates ($k_{app} = 0.44 \pm 0.05\ h^{-1}$) or sonicated β-sheet rich AS fibrils ($k_{app} = 0.47 \pm 0.05\ h^{-1}$) and those corresponding to the spontaneous fibril formation of AS ($k_{app} = 0.41 \pm 0.05\ h^{-1}$), suggesting that the inhibitory interaction of AS and PcTS would mainly take place during the nucleation step. Indeed, the amount of prefibrillar AS species observed at the early stages of the assembly process increases significantly in the PcTS-treated compared with the untreated AS samples (Fig. S1*D*). Together with our EM observations, these data point to a mechanism whereby PcTS might act by trapping prefibrillar AS species during the early stages of the assembly process and interfering with or retarding their progression into amyloid-competent species along the aggregation pathway.

PcTS Inhibition of AS Fibrillation Is Mediated by Binding to the N-Terminal Region. Such interesting features of the antiamyloid activity of PcTS prompted us to explore details of ligand binding to AS by NMR spectroscopy. To analyze the interaction of PcTS with AS, we used ^{1}H-^{15}N heteronuclear single quantum correlation (HSQC) spectra. The ^{1}H-^{15}N HSQC spectrum of a 100 μM sample of uniformly ^{15}N-labeled AS recorded in buffer A at 15 °C is shown in Fig. S2. The resonances were well resolved and sharp, with a limited dispersion of chemical shifts, reflecting the disordered nature and the high degree of mobility of the backbone. Upon titration of ^{15}N-enriched AS with increasing concentrations of PcTS the ^{1}H-^{15}N HSQC spectra retained the excellent resolution of the uncomplexed, native protein, but demonstrated significant broadening and chemical shift changes in a discrete number of residues located at the N-terminal region (Fig. 3*A*). This behavior indicates that a certain number of signals from free and bound states of AS

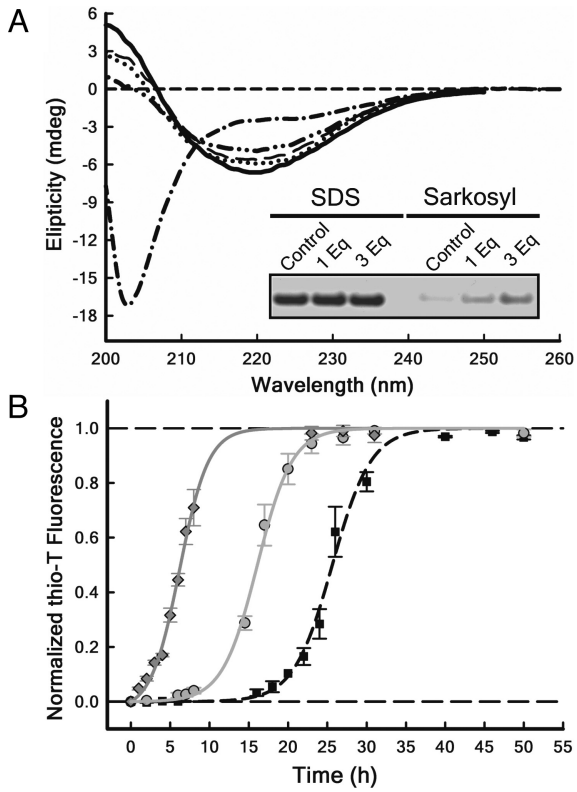

Fig. 2. PcTS inhibition of AS amyloid fibril formation. (*A*) CD spectra of AS incubated for 72 h at 37 °C in the absence (solid line) and presence of one (dotted line), two (dashed line), and three equivalents of PcTS (dashed and double dotted line). The far-UV CD spectrum of unaggregated AS is characteristic of unstructured proteins (dashed and dotted line). The inset shows SDS and Sarkosyl solubilization of pellets from the final point of the aggregation assay, in the absence (control) and presence of one-three equivalents of PcTS. (*B*) Kinetics of AS (100 μM) fibrillation in the absence (black square) and presence of seeds (sonicated AS fibrils (dark gray diamond) or PcTS-generated AS aggregates (light gray circle). The PcTS-generated AS aggregates were obtained by incubation of AS (100 μM) in the presence of 300 μM PcTS.

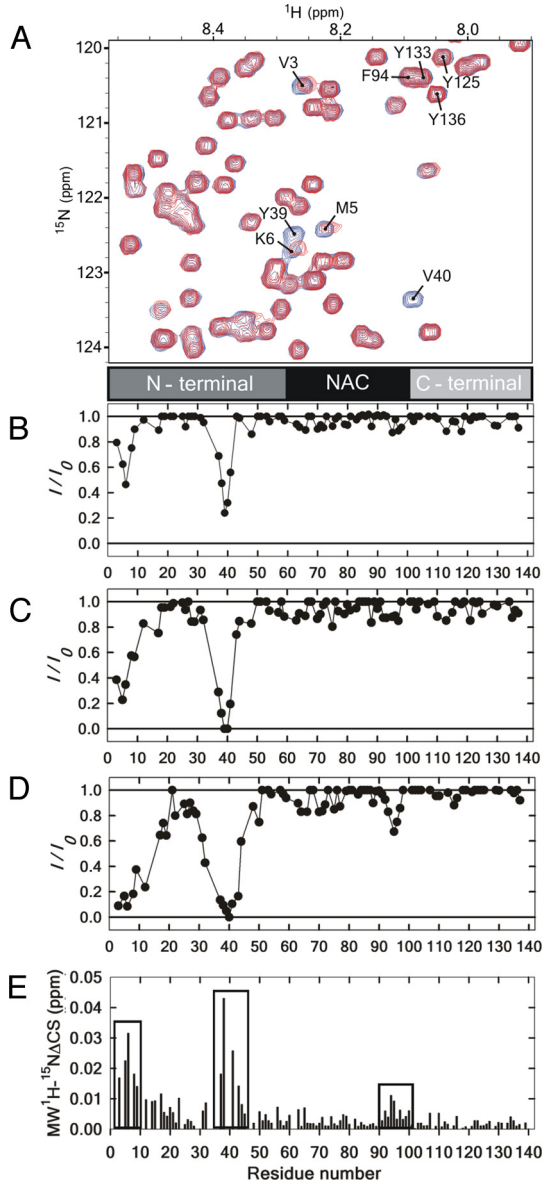

Fig. 3. Analysis of PcTS binding to AS by NMR. (*A*) Overlaid contour plots of ^{1}H-^{15}N HSQC spectra of 100 μM AS in the absence (blue) and presence (red) of 50 μM PcTS. Amino acid residues broadened significantly or beyond detection at the N terminus of AS are identified. For comparative purposes, resonances of aromatic amino acid residues located at the NAC (F94) and C terminus (Y125, Y133, and Y136) are also identified. (*B–D*) I/I_0 profiles of the backbone amide groups of 100 μM AS in the presence of 25 (*B*), 50 (*C*), and 100 (*D*) μM PcTS. (*E*) Differences in the mean weighted chemical shifts (MW^{1}H-^{15}NΔCS) displacements between free and PcTS complexed AS at a molar ratio of 0.5:1 (PcTS:AS).

cannot be resolved and are averaged in a manner that leads to resonance line broadening. Whereas the effects at the N terminus became evident at 25 μM PcTS (Fig. 3*B*), no broadening or chemical shift perturbations were observed under these conditions for the amide groups of residues located in the NAC region or belonging to the C-terminal region. The broadening of resonances at the N terminus was further pronounced at 50–100 μM PcTS (Fig. 3 *C* and *D*), as reflected in values of I/I_0 = 0.2–0.4 for resonances corresponding to residues 3–9 and the broadening beyond detection for signals of residues located in the region 35–41. Interestingly, the amide resonances assigned to the NAC and C-terminal regions remained unaltered at higher PcTS concentrations (100 μM), except by the observation of small broadening and shift perturbation centered in the region 93–95 (Fig. 3 *D* and *E*).

These findings contradict previous research proposing that the inhibitory mechanism of PcTS on AS amyloid formation is mediated by exclusive, specific binding of the compound to the C-terminal region of the protein (21). Moreover, the selective interaction of PcTS with the C-terminal region of AS was further suggested to lead directly to binding between the tetrapyrrolic compound and various synucleins, including BS, and N- and C-terminally truncated species of AS (21). Thus, we also explored the interaction of PcTS with BS and the C-terminal truncated variant of AS (1–108 AS) (Fig. S3 *B* and *C*). The binding features of PcTS complexed to 1–108 AS were similar to those observed on the full length protein, although a stronger effect was observed in the region 93–95 (Fig. S3*C*). The broadening effects on the homologue BS provided evidence for the existence of an additional binding site in this molecule, located in the region encompassing residues 67–73 (Fig. S3*B*). These results allow us to conclude that (*i*) PcTS binds to the native monomeric form of AS; (*ii*) the N-terminal region of AS represents the main PcTS binding interface; (*iii*) the degree of broadening induced by PcTS on AS decreases in the order aa35–41 > aa3–9 ≫ aa93–95; and (*iv*) the transient long-range interactions in AS do not affect the binding preference of PcTS toward the N terminus of the protein, but might hamper the binding to the region 93–95, as observed in C-terminally truncated AS.

Addressing the Nature of AS-PcTS Interactions at the N Terminus. Close analysis of the cross-peaks exhibiting broadening effects on AS upon complexation with PcTS revealed that they correspond to amino acids located in the proximity of aromatic residues; a Phe in position 4 and a Tyr residue in 39 in the regions severely affected at the N terminus; and a Phe in position 94 in the region showing slight broadening at the end of the NAC domain. Comparison between the peak intensity profiles of AS-PcTS and BS-PcTS complexes revealed that the region 67–73, only perturbed in the BS complex, spans the sequence ^{67}GGAVVTG^{73} and ^{67}GGAV**F**SG^{73}, respectively, further suggesting the key role of aromatic side chains in anchoring the ligand to the protein (Fig. 1). Therefore, to investigate the role of aromatic residues in the interaction process, we performed titrations experiments with PcTS on protein variants containing point mutations designed to eliminate binding to one or more of the potential PcTS sites. As shown in Fig. S4 *A–C*, when we studied a mutant of BS lacking the Phe residue in position 71 (F71A), binding of PcTS to the 67–73 region was impaired, proving conclusively the direct involvement of this aromatic residue in the binding of PcTS to that region.

We then studied the mutants F4A, Y39A, and F4A/Y39A of AS, aiming to determine the role of these residues in directing the binding of PcTS to the N terminus (Fig. 4 *A–C*). Complete loss of PcTS binding to the 35–41 region was observed when the Tyr residue in position 39 was replaced by Ala (Fig. 4 *A* and *C*). Conversely, removing the aromatic side chain in position 4 (F4A mutant) was not sufficient to abolish completely PcTS binding to the 3–9 region, as revealed by the presence of a residual binding component at this site (Fig. 4 *B* and *C*). These observations might reflect the involvement of different factors contributing to the binding of PcTS to the N-terminal region. It is likely that electrostatic interactions between the sulfonate groups at the periphery of the core ring of PcTS and positively charged side chains in the amphipathic N terminus of AS might be also implicated in the interaction. To test this possibility, the AS-PcTS complexes were exposed to increasing concentrations of NaCl. Whereas the cross-peaks of residues in the region 3–9 recovered completely their spectral features in the presence of 200 mM NaCl, higher salt concentrations (>400 mM) were necessary to destabilize the AS-

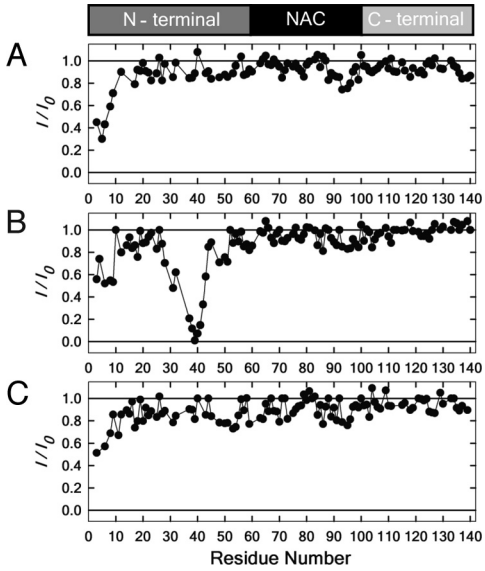

Fig. 4. Analysis of the role of aromatic residues on PcTS binding to the N terminus of AS. I/I_0 profiles of the backbone amide groups of 100 μM protein in the presence of 50 μM PcTS: (*A*) Y39A AS, (*B*) F4A AS, and (*C*) F4A/Y39A AS.

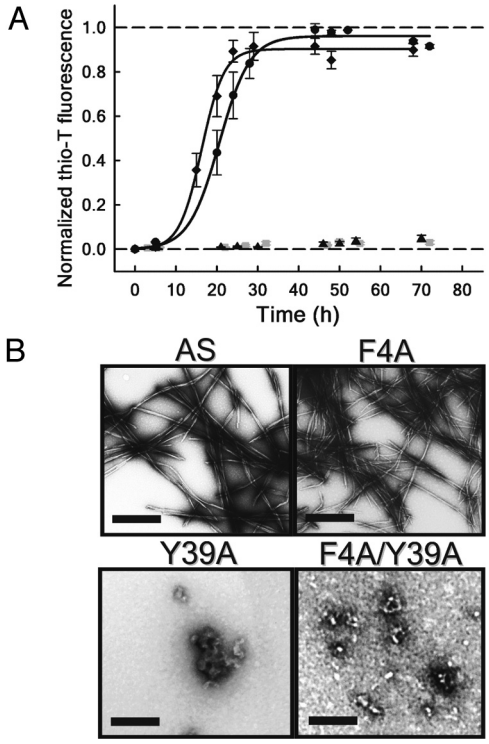

Fig. 5. Tyr 39 has a critical role in the fibrillation pathway of AS. (*A*) Aggregation kinetics of 100 μM AS (black circle), F4A AS (black diamond), Y39A AS (black triangle), and F4A/Y39A AS (light gray square). (*B*) Negative-stain EM images taken at 72 h. [Scale bars, 100 nm.(AS and F4A AS species); 500 nm (Y39A and F4A/Y39A AS species).]

PcTS complex in the region 35–41, encompassing the Tyr residue in position 39 (Fig. S5 *A* and *B*).

Finally, we noted the lack of interaction of PcTS with the cluster of tyrosines located at the C terminus (Y125, Y133, and Y136), which in the light of the previous results might be attributed to electrostatic repulsions between the peripheral sulfonate groups in the ligand and the highly negatively charged C-terminal region. In line with this observation, the long range interactions which position the C terminus of AS close to the central NAC region could then be the reason under the low binding capacity of Phe in position 94.

Altogether, these results demonstrate unequivocally that aromatic residues have a very important role as anchoring moieties for PcTS binding to the N terminus of AS and that the contribution of these interactions to PcTS binding decrease in the order Y39 > F4. Electrostatic interactions, however, do have an auxiliary role as modulators of the interaction, either by attractive or repulsive forces. The fact that point mutations affect only locally the binding features is a demonstration that the identified PcTS sites at positions F4, Y39, and F94 constitute independent, noninteractive binding motifs, consistent with the binding of at least three molecules of PcTS per protein molecule.

Tyr 39 Is the Main Anchoring Residue for PcTS Binding to AS. To gain further insights into the phenomenological determinants of the exchange broadening process monitored by backbone amide resonances, we performed NMR experiments aimed to detect the resonances of aromatic side chains. The distribution of aromatic residues throughout the AS sequence provides excellent probes for exploring the binding features of PcTS to AS. To observe the characteristic ^{1}H and ^{13}C resonances corresponding to the aromatic rings, we performed 1D ^{1}H-NMR and 2D ^{1}H-^{13}C HSQC experiments. Instead of the full length protein, we chose to study the C-terminal truncated species of AS (1–108 AS), because the Tyr-rich C terminus domain does not participate in the binding to PcTS and unnecessarily crowds the spectral region under analysis. The NMR spectra of 1–108 AS in D_2O showed well-resolved clusters of resonances in the 6.0–8.0 ppm (^{1}H) and 115–135 ppm (^{13}C) ranges, comprising the side chains of different aromatic residues: His (aa50), Phe (aa4, aa94), and Tyr (aa39) (Fig. S6 *A* and *D*).

As shown in Fig. S6*B*, the presence of PcTS caused the selective line broadening of the resonances corresponding to the sole Tyr residue. The remaining sharp signals in the cluster centered at 7.1 ppm belong to F4, H50, and F94. Further addition of PcTS caused the Y39 signals to be broadened beyond detection (Fig. S6 *C* and *E*), once more indicative of a system undergoing intermediate exchange on the NMR timescale. The 1D and 2D NMR titration experiments showed that the degree of broadening induced by PcTS on the aromatic side chains of 1–108 AS decrease in the order Y39 > F4 ≫ F94, proving conclusively that Y39 is the primary binding site for this compound in AS. The broadening behavior is consistent with dissociation constants in the low micromolar range for the N-terminal sites (<10 μM) and high micromolar range for the F94 PcTS site (>100 μM), respectively (25). In addition, these results confirm that the broadening observed on the backbone amide groups of AS in the presence of PcTS reflects the interaction of the cyclic tetrapyrrole with aromatic moieties in the protein.

Tyr 39 Has a Critical Role in the Fibrillation Pathway of AS. The combined analysis of the results described above raises the hypothesis that the PcTS-mediated inhibition of AS fibrillation could be linked to the perturbation of essential inter and intramolecular contacts in the protein upon fibril formation. Consequently, we studied the amyloid forming capability of the F4A and Y39A species and of the double mutant F4A/Y39A. As shown in Fig. 5*A*, the $t_{1/2}$ of aggregation of the F4A mutant was comparable with that of the wild-type protein (≈20 h), whereas those species containing the Y39A mutation showed no fibril formation during the entire course of the aggregation experiments (72 h). As determined for the wild-type protein, the formation of amyloid fibrils of the F4A mutant was efficiently inhibited by the addition of PcTS, supporting once more the key role of Y39 in the PcTS-mediated amyloid fibril inhibition. Furthermore, these experiments demonstrate unequivocally that the aromatic side chain of the Tyr residue at position 39 has a critical role in the fibrillation pathway of AS.

Ultrastructural visualization of the protein deposits obtained for the F4A variant using TEM revealed the presence of long, straight fibrils that are morphologically indistinguishable from those formed for the wild-type protein (Fig. 5*B*). In contrast, the TEM images corresponding to the Y39A and F4A/Y39A species showed predominantly nonfibrillar protein structures, similar to those previously described as amorphous AS aggregates in PcTS-treated samples. To further determine whether aggregation of the Y39A containing species occurs with extremely slow kinetics, solutions of these proteins were incubated for 1 week under the same experimental conditions. Similar TEM images were obtained, except by the presence of small amounts of short, flat fibrillar components, an overall picture that resemble the different types of AS structures generated in the presence of PcTS (Fig. S7).

Discussion

Several studies have focused recently on the role of small molecules that interact with AS and inhibit its aggregation-fibrillation in vitro and in vivo (13, 18–24). Despite significant research efforts over the last years, the structural binding details of these compounds have not been established, such that the mechanism(s) by which these compounds inhibit AS amyloid assembly are still poorly understood.

In this work we sought to delineate the structural basis of the interaction between PcTS and AS as a first step toward the understanding of the molecular mechanism by which this compound inhibits AS filament assembly and lead to the formation of nontoxic protein aggregates. The NMR analysis of AS complexes with PcTS indicates that the inhibition of AS amyloid fibril formation in the presence of this compound is a direct consequence of its binding to the N terminus of the protein. The fact that the interaction depends on the presence of the aromatic residues contained in that region demonstrated unequivocally the role of the aromatic moieties as anchoring groups for PcTS binding to AS. Our studies revealed also that electrostatic interactions between negative sulfonates at the periphery of the aromatic ring in PcTS and suitable positioned positive centers on AS, likely provided by lysine residues, contribute differently to the strength of binding on the targeted binding sites. This finding indicates a critical role for other types of bonding such as π-π interactions involving the phthalocyanine aromatic system. Moreover, the region most affected by PcTS binding (^{35}EGVLYVG^{41}) is that implying the higher aromatic character in the interaction (Fig. S5). We therefore propose that specific aromatic interactions with the Y39 residue provide a central mechanistic basis for the inhibitory process of PcTS on AS fibrillation.

The characterization of the interaction between AS and PcTS provided also novel insights into the structural rules that direct the inhibitory mechanism and the potential role of aromatic residues as gate-keepers in the process of amyloid aggregation of AS. A range of small molecules have recently been demonstrated to be capable of inhibiting the formation of fibrillar aggregates for targets such as Aβ, AS, and prion protein. The structural properties of these small molecules contributed to their inhibitory effect, such that their aromatic character was proposed as a key feature to enable interactions with these proteins (11, 26). The inhibitory mechanism proposed would not involve interactions with monomers but rather with higher order amyloidogenic structures, hypothesizing that inhibitor binding might be not sequence-dependent but rather conformation-dependent (26). Instead, the high-resolution structural information shown here demonstrates that PcTS is able to interact with the nonneurotoxic, monomeric state of AS and that the specificity of the binding would be determined by the nature and the location of the amino acid residues in the primary sequence of the protein. Interestingly, the core region of amyloid fibrils of AS was shown to begin somewhere in the range of residues 31–39, in the close vicinity of the primary site targeted by PcTS, and ends around residues 95–109 (27). More recently, NMR and EPR based analysis revealed a tightly-packed region extending from residue 36 to residue 98 (28–30). Thus, the PcTS mediated inhibitory effect would assume specific aromatic interactions in the amyloidogenic sequence of AS, allowing the small molecule to interfere more efficiently with the assembly process.

The inhibitory interaction between PcTS and AS also distinguishes PcTS from other inhibitors of AS assembly reported to act upon the C-terminal region of the protein (13, 24). In addition, many of those small molecules resulted in the formation of SDS-stable AS oligomers (13, 18, 19), indicating that their mechanism of inhibition differs significantly from that of PcTS. We have found here that the inhibitory interaction of AS and PcTS would mainly take place during the nucleation step. Indeed, the fact that the residue 39 was found to be solvent-exposed in the monomer but also in transient species formed during the early stages of AS fibrillation (31) implies that Y39 could be also targeted directly by PcTS in early aggregate AS species. The proposed mechanism behind the AS-PcTS inhibitory interaction might be then correlated to the trapping of assembly-competent species involved in the dynamic equilibrium between monomers and the nucleation reaction, preventing their progression into amyloid-competent species along the aggregation pathway.

The AS variants designed on the basis of the interaction with PcTS support also a critical role for Y39 in the fibrillation pathway of AS and into the mechanistic rules directing the inhibitory effect of PcTS. The implication of tyrosine residues on AS aggregation has been explored recently by mutagenesis-based approaches (32, 33). A study based on tyrosine-to-cysteine modified AS revealed that cysteine substitution in the Y39 but not in the Y125, Y133, and Y136 positions preferentially enhanced dimer and oligomer formation under oxidative conditions, suggesting a dimerization pathway mediated by this region (32). Another study reported that substitution of Tyr-39 and Tyr-133 by Ala resulted in substantial inhibition of fibrillation, suggesting that Tyr-39 and the C-terminal Tyr residues might form an aromatic cluster that stabilizes the native state of AS (33). Our NMR experiments on the Y39A mutant reveal that the changes induced by the mutation are only local and restricted to the immediate vicinity of the Tyr residue (Fig. S8), an evidence that indicates that the substantial change of aggregation rate after mutation of Y39 would be hence fully attributable to a loss of function of the aromatic side chain in the self-assembly process rather than on the conformational destabilization of the native state.

The fact that PcTS inhibition of AS amyloid fibril formation is mediated via specific binding to the N-terminal region of the protein and the identification of the interactions and mechanistic basis contributing to their inhibitory effect constitute important findings of this work, supporting a key role for aromatic moieties in amyloid formation. At this juncture a tighter link with other proteins involved in amyloid-related disorders can be sought, based on these new insights into the structural basis of PcTS interactions with AS. Besides the inhibitory activity of porphyrins on Aβ aggregation (10), the NMR features of the AS-PcTS complexes resembled that observed for the interaction between Aβ and PcTS, in which aromatic residues Y10 and F19-F20 resulted strongly affected and broadened beyond detection (34). Interestingly, the stretch F19-F20 is well-known to modulate the assembly of Aβ (35). Inhibition of tau filament formation by porphyrin compounds has been also documented. A recent study have identified two hexapeptides located around the second and third repeat sequences in the core region of the protein that were shown to represent a minimal tau-tau interaction motif and be sufficient for the formation of the characteristic paired helical filaments (36). Interestingly, one of the occurring hexapeptides corresponds to the sequence VQIVYK, which at the light of our findings might represent the target for the inhibitory effect mediated by cyclic tetrapyrroles on tau filament assembly. Thus, added to the fact that cyclic tetrapyrroles have been shown to block different types of disease-associated protein aggregation, our studies raise the possibility that these compounds might have similar mechanisms of action in slowing the formation of a variety of pathological aggregates.

The new findings reported here underscore the use of aggregation inhibitors as molecular probes to assess structural and toxic mechanisms related to amyloid formation. Furthermore, because the structural basis for the aggregation inhibitory mechanism of these compounds is starting to emerge, structural optimization of small molecule inhibitors for therapeutic effectiveness is especially promising.

Materials and Methods

Proteins and Reagents. Unlabeled and ^{15}N-labeled AS and BS species were prepared as previously described (6). The F4A, Y39A, and F4A/Y39A AS and F71A BS mutants were constructed using the Quick-Change site directed mutagenesis kit (Stratagene) on the AS and BS sequence containing plasmids. The introduced modifications were further verified by DNA sequencing. Purified proteins were dialyzed against buffer A (20 mM Mes, 100 mM NaCl, pH 6.5) supplemented with Chelex (Sigma). PcTS was purchased from ICN Biomedical Inc.. $^{15}NH_4Cl$, ^{13}C-glucose, deuterated Mes buffer, and deuterium oxide (D_2O) were from Cambridge Isotope Laboratories.

Aggregation Assays. Aggregation kinetics measurements were performed with 100 μM protein samples dissolved in buffer A. Samples were incubated at 37 °C under constant stirring. The formation of fibrils was estimated from aliquots (5 μL) taken at different time points by use of the thioflavin-T fluorescence assay (6). For seeding experiments, PcTS generated AS aggregates or sonicated β-sheet rich AS fibrils [2% (vol/vol)] were added to the aggregation reactions. Aggregation yields were normalized to the final values and the averaged data points were fitted according to ref. 6. In all cases, the reported values correspond to the average of at least five independent aggregation measurements.

The amount of soluble AS monomers at the initial and end points of the aggregation assay were determined by integration of the protein NMR resonances in the aliphatic region of the 1D ^{1}H-NMR spectrum (0.4–2.1 ppm). For the sedimentation analysis in Fig. S1*A*, aliquots withdrawn from the aggregation assay were centrifuged at 16,000 $\times$ *g* for 10 min. Supernatant fractions, indicative of soluble protein, were resolved by SDS/PAGE and stained with Coomassie Blue.

For the detergent-sensitivity studies, aliquots withdrawn from the aggregation assay were centrifuged at 16,000 $\times$ *g* for 10 min. Pellet fractions were incubated for 30 min in 1% Sarkosyl, and the solubilized material were resolved by SDS/PAGE and stained with Coomassie Blue.

CD and Electronic Absorption Spectroscopy. AS samples were aggregated as described above, in the absence and presence of 100–300 μM PcTS. Samples were diluted 20-fold in buffer A, and CD spectra were recorded on a JASCO J-800 spectropolarimeter. Visible electronic absorption spectra of the supernatant and pellet fractions from the PcTS generated AS aggregates were obtained on a JASCO V-550 spectrophotometer.

NMR Spectroscopy. NMR spectra were acquired on a Bruker Avance II 600-MHz spectrometer using a triple-resonance probe equipped with *z* axis self-shielded gradient coils. Heteronuclear NMR experiments were performed with pulsed-field gradient enhanced pulse sequences on 100 μM ^{15}N-labeled or 200 μM ^{13}C-labeled protein samples in buffer A, at 15 °C. One-dimensional ^{1}H-NMR experiments were acquired at 15 °C on 400 μM unlabeled AS dissolved in deuterated buffer A. Aggregation did not occur under these low temperature conditions and absence of stirring.

For the mapping experiments, ^{1}H-^{15}N HSQC amide cross-peaks affected during PcTS titration were identified by comparing their intensities (I) with those of the same cross-peaks in the dataset of samples lacking the tetrapyrrolic compound (I_0). The I/I_0 ratios of 95–105 nonoverlapping cross-peaks were plotted as a function of the protein sequence to obtain the intensity profiles. Mean weighted chemical shifts displacements (MW^{1}H-^{15}NΔCS) were calculated as $[(\Delta\delta^1\mathrm{H})^2 + (\Delta\delta^{15}\mathrm{N})^2/25]^{1/2}$. Acquisition, processing, and visualization of the spectra were performed by using TOPSPIN 2.0 (Bruker), NMRPipe (37), and Sparky.

Electron Microscopy. Ten-microliter aliquots withdrawn from aggregation reactions were adsorbed onto Formvar/carbon-coated copper grids (Agar Scientific) and negative stained with 2% (wt/vol) uranyl acetate. Images were obtained at various magnifications (1,000–90,000$\times$) using a Philips CEM100 TEM.

ACKNOWLEDGMENTS. We thank A. J. Vila and R. M. Rasia for useful discussions. C.O.F. is the head of a Partner Group of the Max Planck Institute for Biophysical Chemistry. This work was supported by Agencia Nacional de Promoción Científica y Tecnológica (ANPCyT), Fundación Antorchas, Consejo Nacional de Investigaciones Científicas y Técnicas (CONICET), Max Planck Society, and Alexander von Humboldt Foundation (C.O.F.); a fellowship from CONICET in Argentina (A.B. and G.R.L.); Fundación Josefina Prats (G.R.L. and C.O.F.); a fellowship from ANPCyT in Argentina (M.L.O.); an EMBO long-term fellowship (C.W.B.); and the Deutsche Forschungsgemeinschaft Heisenberg Scholarship ZW 71/2-1 and 3-1 (to M.Z.). The Bruker Avance II 600-MHz NMR spectrometer used in this work was purchased with funds from ANPCyT (PME2003–2006) and CONICET.

1. Luheshi LM, Crowther DC, Dobson CM (2008) Protein misfolding and disease: From the test tube to the organism. *Curr Opin Chem Biol* 12:25–31.
2. Spillantini MG, et al. (1997) α-Synuclein in Lewy bodies. *Nature* 388:839–840.
3. Polymeropoulos MH, et al. (1997) Mutation in the α-synuclein gene identified in families with Parkinson's disease. *Science* 276:2045–2047.
4. Kruger R, et al. (1998) Ala30Pro mutation in the gene encoding α-synuclein in Parkinson's disease. *Nat Genet* 18:106–108.
5. Giasson BI, Murray IV, Trojanowski JQ, Lee VM (2001) A hydrophobic stretch of 12 amino acid residues in the middle of α-synuclein is essential for filament assembly. *J Biol Chem* 276:2380–2386.
6. Fernandez CO, et al. (2004) NMR of α-synuclein-polyamine complexes elucidates the mechanism and kinetics of induced aggregation. *EMBO J* 23:2039–2046.
7. Lee JC, Gray HB, Winkler JR (2005) Tertiary contact formation in α-synuclein probed by electron transfer. *J Am Chem Soc* 127:16388–16389.
8. Bertoncini CW, et al. (2005) Release of long-range tertiary interactions potentiates aggregation of natively unstructured α-synuclein. *Proc Natl Acad Sci USA* 102:1430–1435.
9. Lee JC, Lai BT, Kozak JJ, Gray HB, Winkler JR (2007) α-Synuclein tertiary contact dynamics. *J Phys Chem B* 111:2107–2112.
10. Howlett D, Cutler P, Heales S, Camilleri P (1997) Hemin and related porphyrins inhibit beta-amyloid aggregation. *FEBS Lett* 417:249–251.
11. Frydman-Marom A, et al. (2008) Cognitive-performance recovery of Alzheimer's disease model mice by modulation of early soluble amyloidal assemblies. *Angew Chem Int Ed* 47:1–7.
12. Necula M, Kayed R, Milton S, Glabe CG (2007) Small molecule inhibitors of aggregation indicate that amyloid beta oligomerization and fibrillization pathways are independent and distinct. *J Biol Chem* 282:10311–10324.
13. Ehrnhoefer DE, et al. (2008) EGCG redirects amyloidogenic polypeptides into unstructured, off-pathway oligomers. *Nat Struct Mol Biol* 15:558–566.
14. Taniguchi S, et al. (2005) Inhibition of heparin-induced tau filament formation by phenothiazines, polyphenols, and porphyrins. *J Biol Chem* 280:7614–7623.
15. Chopra V, et al. (2007) A small-molecule therapeutic lead for Huntington's disease: Preclinical pharmacology and efficacy of C2–8 in the R6/2 transgenic mouse. *Proc Natl Acad Sci USA* 104:16685–16689.
16. Caughey WS, Raymond LD, Horiuchi M, Caughey B (1998) Inhibition of protease-resistant prion protein formation by porphyrins and phthalocyanines. *Proc Natl Acad Sci USA* 95:12117–12122.
17. Priola SA, Raines A, Caughey WS (2000) Porphyrin and phthalocyanine antiscrapie compounds. *Science* 287:1503–1506.
18. Masuda M, et al. (2006) Small molecule inhibitors of α-synuclein filament assembly. *Biochemistry* 45:6085–6094.
19. Masuda M, et al. (2009) Inhibition of α-synuclein fibril assembly by small molecules: Analysis using epitope-specific antibodies. *FEBS Lett* 583:787–791.
20. Zhu M, et al. (2004) The flavonoid baicalein inhibits fibrillation of α-synuclein and disaggregates existing fibrils. *J Biol Chem* 279:26846–26857.
21. Lee EN, et al. (2004) Phthalocyanine tetrasulfonates affect the amyloid formation and cytotoxicity of α-synuclein. *Biochemistry* 43:3704–3715.
22. Rao JN, Dua V, Ulmer TS (2008) Characterization of α-synuclein interactions with selected aggregation-inhibiting small molecules. *Biochemistry* 47:4651–4656.
23. Hong DP, Fink AL, Uversky VN (2008) Structural characteristics of α-synuclein oligomers stabilized by the flavonoid baicalein. *J Biol Chem* 383:214–223.
24. Norris EH, et al. (2005) Reversible inhibition of α-synuclein fibrillization by dopaminochrome-mediated conformational alterations. *J Biol Chem* 280:21212–21219.
25. Cavanagh J (2007) in *Protein NMR Spectroscopy, Principles and Practice*, eds Cavanagh J, Fairbrother WJ, Palmer AG, Rance M, Skelton NJ (Academic, London), 2nd Ed, pp 725–780.
26. Porat Y, Abramowitz A, Gazit E (2006) Inhibition of amyloid fibril formation by polyphenols: Structural similarity and aromatic interactions as a common inhibition mechanism. *Chem Biol Drug Des* 67:27–37.
27. Der-Sarkissian A, Jao CC, Chen J, Langen R (2003) Structural organization of α-synuclein fibrils studied by site-directed spin labeling. *J Biol Chem* 278:37530–37535.
28. Heise H, et al. (2005) Molecular-level secondary structure, polymorphism, and dynamics of full-length α-synuclein fibrils studied by solid-state NMR. *Proc Natl Acad Sci USA* 102:15871–15876.
29. Chen M, Margittai M, Chen J, Langen R (2007) Investigation of α-synuclein fibril structure by site-directed spin labeling. *J Biol Chem* 282:24970–24979.
30. Vilar M, et al. (2008) The fold of α-synuclein fibrils. *Proc Natl Acad Sci USA* 105:8637–8642.
31. Dusa A, et al. (2006) Characterization of oligomers during α-synuclein aggregation using intrinsic tryptophan fluorescence. *Biochemistry* 45:2752–2760.
32. Zhou W, Freed CR (2004) Tyrosine-to-cysteine modification of human α-synuclein enhances protein aggregation and cellular toxicity. *J Biol Chem* 279:10128–10135.
33. Ulrih NP, Barry CH, Fink AL (2008) Impact of Tyr to Ala mutations on α-synuclein fibrillation and structural properties. *Biochim Biophys Acta* 1782:581–585.
34. Yao S, Cherny RA, Bush AI, Masters CL, Barnham KJ (2004) Characterizing bathocuproine self-association and subsequent binding to Alzheimer's disease amyloid beta-peptide by NMR. *J Pept Sci* 10:210–217.
35. Tjernberg LO, et al. (1999) A molecular model of Alzheimer amyloid beta-peptide fibril formation. *J Biol Chem* 274:12619–12625.
36. von Bergen M, et al. (2000) Assembly of tau protein into Alzheimer paired helical filaments depends on a local sequence motif ((306)VQIVYK(311)) forming beta structure. *Proc Natl Acad Sci USA* 97:5129–5134.
37. Delaglio F, et al. (1995) NMRPipe: A multidimensional spectral processing system based on UNIX pipes. *J Biomol NMR* 6:277–293.